Structure versus Solvent Effects on Nonlinear Optical Properties of Push−Pull Systems: A Quantum-Mechanical Study Based on a Polarizable Continuum Model†

Alessandro Corozzi,‡ Benedetta Mennucci,‡ Roberto Cammi,§ and Jacopo Tomasi*,‡

Dipartimento di Chimica e Chimica Industriale, Università di Pisa, Via Risorgimento 35, 56126 Pisa, and Dipartimento di Chimica, Università di Parma, Viale delle Scienze 17/A, 43100 Parma

Received: May 26, 2009; Revised Manuscript Received: August 24, 2009

A quantum mechanical investigation on the effects of the solvent and the structure on nonlinear optical activity of a class of merocyanine compounds has been conducted. The interplay of the two effects on the first hyperpolarizability, computed at density functional theory and second-order Møller−Plesset level, has been analyzed in combination with ground state properties and geometries and excited state energies and dipoles. A critical analysis of the simplified two-level model has also been presented.

1. Introduction

A large part of the present nonlinear optics (NLO) research is focused on two interconnected lines, the design and the synthesis of new organic molecules and the quantum-mechanical interpretation of their structure-properties relationship.

Organic molecules are easy to manipulate, they can be crystallized, they are robust, and they can be incorporated into plastics. In addition, the power of the organic chemistry to tailor materials at will gives us the possibility to synthesize molecules with larger nonlinear optical effects than in traditional inorganic materials.[1] In particular, in the last years great attention has been focused on a specific type of organic molecules as potential efficient NLO chromophores, the push−pull molecules characterized by a polarizable π-electron system and donor and acceptor groups to create an asymmetric polarizability.[2−5] Generally, in push−pull molecules, a simple but effective model is introduced to rationalize their electronic behavior and in particular their hyperpolarizability β, a fundamental property to design efficient NLO materials. According to this model, known as two-level model (TLM),[6−9] the dominant contribution to β arises from the ground state and a charge-transfer (CT) excited state and as a result the common definition of β in terms of sum over all excited state reduces to a single term corresponding to the CT state. In parallel, both ground and excited states are represented in terms of two resonance limit forms showing a neutral and a zwitterionic character, respectively. By modulating the relative weight of the two forms a very different behavior can be induced in the systems with corresponding enhancement (or depletion) of the NLO activity. A common way to control such a nonlinear optical response is to increase the electronic asymmetry of the molecule, and this is generally done by changing the relative strengths of the donor and acceptor groups. A further factor that can strongly influence the NLO properties is the polarity of the solvent; its influence when cooperatively combining with a proper structural design can in fact lead to an extraordinarily variable range of β values, eventually switching from negative to positive.

In this work, the focus is on a class of highly polarizable merocyanine compounds originally synthesized and characterized by Abbotto et al.[10] It is a family of azinium-(CH=CH-thyenil)-dicyanomethanido chromophores in which the presence of electron-donor and electron-acceptor terminal groups linked by a π-conjugated chain makes them a clear example of push−pull molecules (see the scheme below for the indication of the structures and the short names we will use in the following).

In this class of chromophores, the modulation of the intramolecular charge transfer is governed by consecutive annelation of the pyridyl ring. This annelation effect can in fact cause significant bond alternation and influence the relative importance of the aromatic/quinoid character of the azinium ring. In particular, a tuning of the charge transfer can be obtained by changing the environment; moving from apolar to polar solvents has shown to largely affect the NLO activity of these systems.

To rationalize this delicate interplay between solvent and structural changes quantum-mechanical (QM) methods that include electron correlation and solvation models which properly account for the details of the structural and the charge distribution of the solute are required.

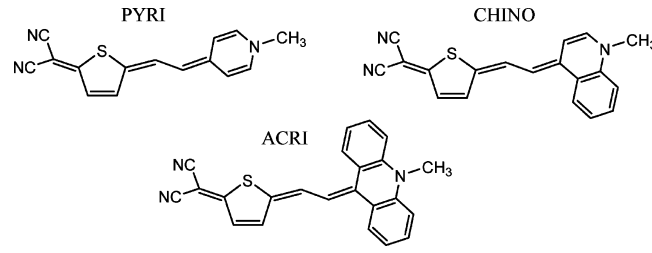

As far as concerns accurate QM methods for NLO properties, a fundamental contribution came from the development of response theories,[11] and their extension to correlated levels of theories (such as second-order Møller−Plesset, MP2, and coupled cluster); these in fact have shown to reproduce molecular hyperpolarizabilities with good accuracy.[12] More recently, density functional theory (DFT) methods have started to be widely used to evaluate NLO properties; however the accuracy that can be achieved at this level of theory is still an open probem.[13,14] Inadequacies of pure DFT functionals both in the local density approximation and the generalized gradient approximation (GGA) were identified as wrong asymptotic behavior of the functional and self-interaction error. Since these

† Part of the "Vincenzo Aquilanti Festschrift".
* To whom correspondence should be addressed.
‡ Università di Pisa.
§ Università di Parma.

10.1021/jp904906n
Published on Web 09/23/2009

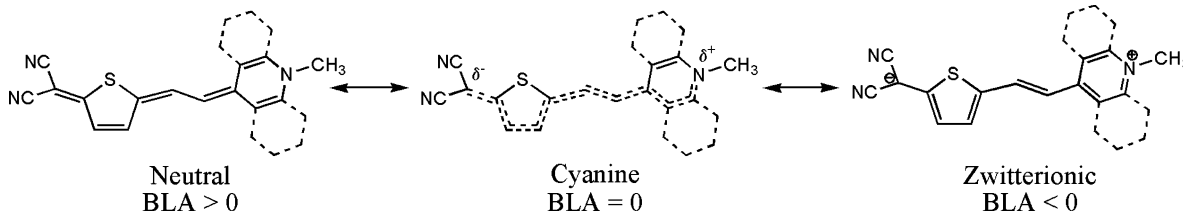

Figure 1. Pictorial representation of the dependence of the neutral/zwitterionic character on BLA

sources of error are absent in HF method, the fraction of HF exchange introduced in hybrid functionals reduces but does not completely eliminate the inaccuracies of pure DFT.

Moving to the description of solvent effects on both structure and NLO properties, it is known that an accurate consideration of the geometrical structure and of the charge distribution of the dye are important aspects to properly model the solvent effects on molecular response properties. Nowadays, there are many alternative solvation models that can be used. However, among the available approaches, the most popular for this kind of study is still represented by continuum solvation models.[15,16] Within the framework of semiclassical descriptions, important applications to NLO properties have been made by Wortmann and Bishop[17] and by Ågren and co-workers.[18] Quantum mechanical descriptions of the effect of the solvent on NLO properties have been carried out by, among others, Willets and Rice,[19] Yu and Zerner,[20] and Mikkelsen and co-workers.[21] Still within the quantum-mechanical approaches, the polarizable continuum model (PCM) developed in Pisa[22,23] has shown to be an effective approach to study several linear and nonlinear optical processes in liquid phase.[24] Within this method, in fact, the optical property of interest is obtained by introducing into a response equation scheme[25] the proper terms representing the interaction with both the solvent reaction field and the Maxwell field in the medium, thus leading to an ab initio evaluation of the corresponding macroscopic susceptibilities.

In the present work, a detailed investigation of both aspects is performed by using DFT and MP2 descriptions in combination with PCM for the solvent effect. In such a way, structure and solvents effects on β will be analyzed comparing TLM estimates with finite-field (FF) calculations. In addition, UV−vis absorption wavelengths and NMR chemical shifts are calculated and compared with experiments. All calculated data have been analyzed in terms of possible correlations with structural and charge parameters.

The paper is organized as follows. In Section 2, a description of the computational strategy used is presented; in Section 3, the results obtained are presented and compared with experiments; and in Section 4, conclusive comments are reported.

2. Computational Details

Because of the problems shown by DFT in correctly describing bond length alternation in highly conjugated systems,[13,26] for all molecules in all different environments ground state geometries have been obtained at two different levels of QM theory, namely B3LYP[27] and MP2 (6-31+G(d) and 6-31G(d) basis sets have been used in two methods, respectively).

Electronic excitation energies and the corresponding transition dipoles have been obtained using the time dependent density functional theory (TDDFT)[26] with the 6-31+G(d) basis set. For common local excitations, the B3LYP functional gives electronic excitation energies similar to highly correlated methods. However, when B3LYP is used to study charge-transfer excitations in organic push−pull π-conjugated systems, the accuracy of the results is generally reduced in an unpredictable way.[29] One of the main reasons for such an unpredictable behavior is due to the incorrect asymptotic behavior of the exchange contribution to the Kohn−Sham equations. This possible limitation gets worse if the dimension of the system is increased, especially the length of the π-conjugated bridge connecting donor and acceptor groups. One approach that has shown to be promising for improving the accuracy of CT excitations while maintaining good quality local excitations is to partition the $1/r_{12}$ operator in the exchange term into short- and long-range components.[30] Among this class of new functionals, a quite successful one is the Coulomb-attenuated CAM-B3LYP.[31] The same functional has been successfully used to calculate linear and nonlinear optical properties.[32] For these reasons, CAM-B3LYP has been selected as more accurate alternative to B3LYP in the present study and used both in the TLM and FF approach in combination with a 6-31+G(d) basis set. To check the reliability of the basis set, some tests on the PYRI system have been done using 6-311+G(d) and 6-311++G(d,p). As a further correlated method, MP2/6-31G(d) has been also used in the calculation of the FF hyperpolarizabilities.

In all calculations, solvent effects have been modeled using the integral equation formalism (IEF) version of PCM.[23] In such a model, the solute molecule, which is assumed to be hosted in a cavity inside a polarizable continuum dielectric representing the solvent, is treated quantum mechanically, whereas the solvent polarization is described in terms of an induced surface charge on such a cavity. The shape of the cavity is obtained as the envelope of spheres centered on selected atoms of the solute and is thus determined by the solute geometry. In the present case, we have used cavities constructed by applying the united atom topological model and the atomic radii of the UFF[33] force field as implemented in the GAUSSIAN code.[34] According to this model, a sphere is associated to each atom (excluding the hydrogens) with radii defined according to the type of atom and the bonds; namely we have R(CH) = 2.125, R(C) = 1.925, R(N) = 1.83, R(S) = 2.017, and R(CH_3) = 2.525 (all values are in Å).

To describe the solvent response, the following dielectric constants have been used: dioxane 2.21, $CHCl_3$ 4.80, DMF 36.70, and DMSO 46.70. In the case of polar solvents, the optical components of the dielectric constant used are $CHCl_3$ 2.085, DMF 2.04, and DMSO 2.18.

All calculated results have been obtained using a local version of the Gaussian software package.[34]

3. Results

The presentation and discussion of the results is organized in four sections, focused on ground state geometries, NMR chemical shifts, UV absorption spectra, and TLM and FF static hyperpolarizabilities.

3.1. Bond Length Alternation (BLA). The combined effect of BLA, which strictly depends upon the π-electron structure,

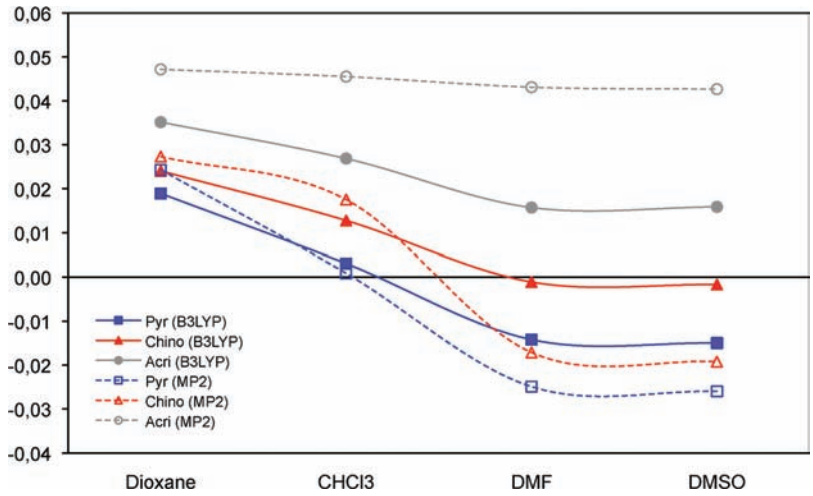

Figure 2. Solvent effects on BLA values for the three systems. Full lines refer to B3LYP optimizations and dotted lines to MP2 optimizations.

and of solvent influences the change in the relative contributions of the two neutral and dipolar limit forms generally used to describe ground and excited states (see Figure 1 for a pictorial representation of such a dependence).

In the investigated systems, the definition of BLA is not univocal. Looking at Figure 1, a working definition of BLA is that including all the bonds (including the final C−N bond) that are involved in the possible single-to-double bond change passing from the neutral to the zwitterionic form. In Figure 2, the solvent dependence of the BLA of the three systems is shown both at B3LYP and MP2 level. As a further useful piece of information, we recall that only the PYRI system presents a planar structure while both CHINO and ACRI systems show strong deformation from planarity in the azinium group.

Looking at Figure 1, it appears evident that in the PYRI system the neutral limit form corresponds to a loss of aromaticity (i.e., a quinoid structure); this should be disfavored with respect to the zwitterionic (and aromatic) form. As a result, a negative BLA is expected especially in polar solvents. From Figure 2, it can be noticed that this prediction is correctly reproduced by both DFT and MP2 methods. In both cases, BLA crosses zero between $CHCl_3$ and DMF even if the range of values is much smaller for B3LYP than for MP2.

Also for the CHINO system, B3LYP and MP2 both show a change of sign between $CHCl_3$ and DMF but for this system the negative values found in polar solvents are quite small showing that the contribution of the zwitterion form is less important than in the PYRI system. This is particularly evident at B3LYP level.

Finally, moving to the ACRI system, both at B3LYP and MP2 level, BLA is always positive and large (especially at MP2 level); this means that a neutral structure is dominant whatever is the solvent. This result can be explained observing that for this system a high ring aromaticity acts against the π-conjugation along the chain and it can better sustain a neutral (or quinoid) character.

This analysis shows that B3LYP and MP2 give quite different pictures of BLA passing from PYRI to ACRI system (and from apolar to polar solvents). These differences in the description of the sensitivity of the three systems to structural and solvent effects are expected to have important implications in the successive study of NLO properties and they worth a further analysis.

3.2. NMR Spectra. To better appreciate the reliability of the geometries obtained either with B3LYP and MP2, we have calculated NMR ^{13}C spectra. It is in fact well known that geometry changes can have a strong correlation with variations of magnetic properties such as chemical shifts. Here, in particular we compare B3LYP/GIAO (gauge independent atomic orbital)[35] chemical shifts of the three systems as obtained using B3LYP and MP2 optimized geometries. As experimental data are available only for DMSO as solvent, also the calculations have been limited to this single solvent.

Experimental and B3LYP/6-311+G(2d,p) chemical shifts of the carbons of the main backbone structure for the three systems in DMSO are shown in Figure 3.

A general good agreement between calculated and experimental data are found both in terms of trends and absolute values. The results do not significantly depend on the geometry; using either B3LYP or MP2 optimized structures, the average error is less than 10% for all nuclei with the exception of the carbon atoms on the thiophene ring for which larger errors are found.

The comparison with the available ^{15}N data is more difficult. While it has been shown that carbon nuclear shieldings can be accurately described by standard functionals such as B3LYP with extended basis sets as the ones used here, nitrogen is still a less studied nucleus and no well-defined computational protocols have been proposed. We have thus decided to use the same functional and basis set used for C also to calculate N nuclear shieldings. Experimental data are known only for the azinium nitrogen in DMSO; we also note that the experimental data refer to systems not exactly equivalent to those used in the calculations; for PYRI and CHINO measured data refer to a nitrogen atom linked to a $nC_{10}H_{21}$ group while for ACRI system they refer to N(H). The calculated data show an error of 4% for PYRI using either DFT or MP2 geometries, 7% (DFT) and 11%(MP2) for CHINO, and a large error (30% at both DFT and MP2 geometries) for ACRI. This much larger error for ACRI can surely be imputed to the presence of a linked H in the experimental system; this in fact will change the electronic charge distribution on nitrogen and can also have hydrogen-bonding interactions with DMSO which indirectly affect the nuclear shielding of the nitrogen.

Both the analysis on carbon and nitrogen shieldings show that such NMR data do not present a sufficient sensitivity to the details of the geometrical structure to allow a validation of the calculated geometries, and the following selection between DFT and MP2. However, the general good agreement found

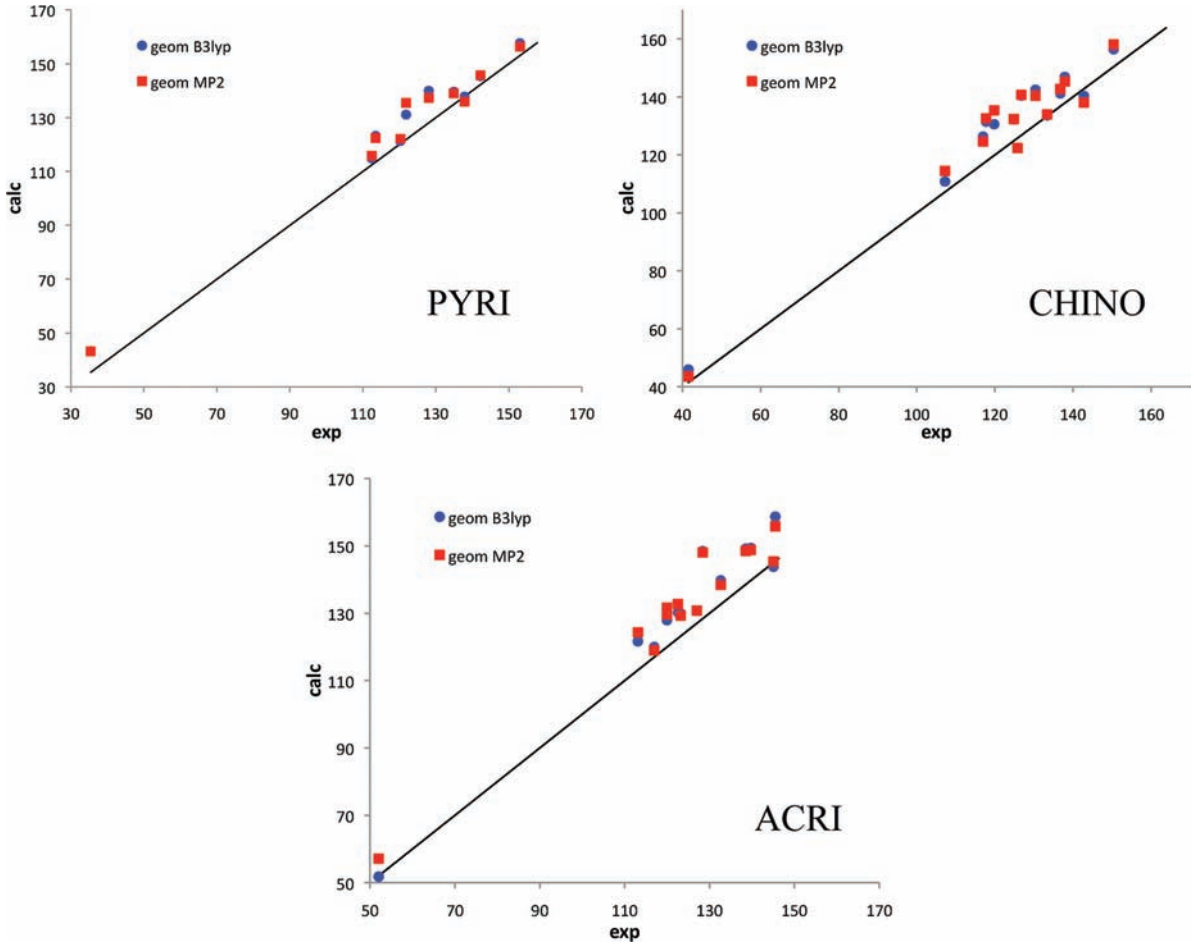

Figure 3. Correlation between B3LYP/6-311+G(2d,p) and experimental[10] ^{13}C chemical shifts for the PYRI, CHINO, and ACRI systems in DMSO. Tetramethylsilane is the reference molecule chosen in both experimental and computational data.

TABLE 1: Experimental and Calculated Absorption Energies of the Three Investigated Systems in Different Solvents[a]

		TDB3LYP		TDCAMB3LYP	
geom	exp	B3LYP	MP2	B3LYP	MP2
		PYRI			
DMSO	2.04 (0.29)	2.20 (0.02)	2.20 (0.01)	2.34 (0.16)	2.40 (0.20)
$CHCl_3$	1.81 (0.06)	2.17 (−0.01)	2.17 (−0.02)	2.21 (0.02)	2.21 (0.02)
dioxane	1.75	2.18	2.19	2.19	2.20
		CHINO			
DMSO	1.78 (0.12)	2.04 (−0.04)	1.99 (−0.06)	2.13 (0.01)	2.21 (0.12)
$CHCl_3$	1.66 (0.00)	2.03 (−0.05)	2.05 (−0.01)	2.05 (−0.07)	2.08 (−0.01)
dioxane	1.66	2.08	2.06	2.13	2.09
		ACRI			
DMSO	1.58 (−0.39)	1.95 (−0.07)	2.00 (−0.06)	2.01 (−0.14)	2.16 (−0.10)
$CHCl_3$	1.88 (−0.08)	1.98 (−0.04)	2.03 (−0.03)	2.07 (−0.07)	2.21 (−0.05)
dioxane	1.97	2.02	2.06	2.15	2.25

[a] In parentheses the solvatochromic shift with respect to dioxane is reported. All values are eV.

with experiments passing from one system to the other, makes us confident on the coherent description obtained for the three systems.

3.3. UV−vis Spectra. Once we have determined and analyzed changes in the geometry due to the combination of structural and solvent effects, we move to verify how these effects are reflected in the electronic properties. As indicated in the computational details, here we adopt a TDDFT approach to study electronically excited state and to evaluate both their transition and state properties. The latter are calculated in terms of the relaxed density, which can be obtained thanks to the extension of TDDFT to analytical gradients.[36] This extension has been recently generalized to include PCM solvent effects.[37,38]

Experimental and calculated excitation wavelengths are reported in Table 1. Experimental data refer to band maxima.

As in the present analysis, the interest is mainly focused on the combined effect of structure and solvent, the data reported in Table 1 will be commented in terms of shifts. We note that in principle this a more fair analysis when TDDFT excitation energies are compared with experiments. In fact, as we have already said, TDDFT is not an extremely accurate approach to study CT excited states (even in its most recent formulations

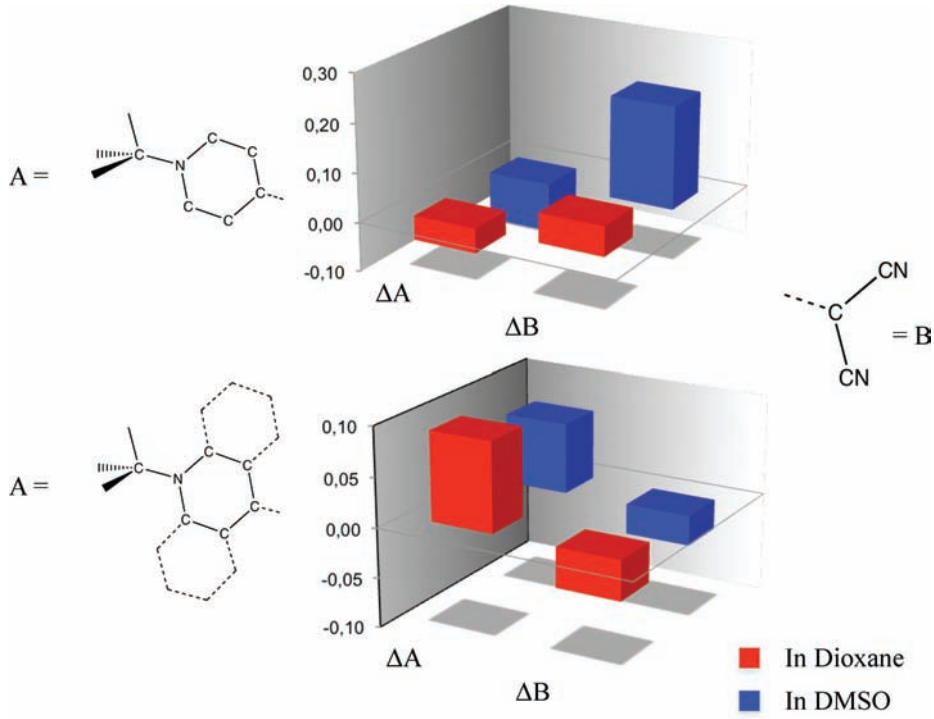

Figure 4. Changes in the MK charges of the terminal groups A and B passing from ground to excited state for pyridinic (upper graph) and acridinic system (lower graph) in dioxane (red boxes) and DMSO (blue boxes). Only TD-CAMB3LYP results at MP2 geometries are reported.

in terms of new functionals). However, in order to have a meaningful study, we have to expect that trends passing from one system to the other and/or from a solvent to the other, are correctly reproduced.

As it can be seen from Table 1, by increasing solvent polarity a very different response is observed in the different systems, namely a blue shift for PYRI and CHINO systems and a red shift for the ACRI system. These opposite shifts are correctly described at TDCAMB3LYP level (at MP2 geometries) whereas TDB3LYP generally gives a much worse description especially for the larger systems.

As expected, the effect of the different geometry (either B3LYP or MP2) becomes quite important for the two larger systems, that is, for the systems for which we found the largest differences in the prediction of the BLA (see Figure 2); this is particularly evident at TDCAMB3LYP level. In fact, if we focus on the solvatochromic shift DMSO−Diox, we can see that for PYRI system there is a relatively small increase in the magnitude of the shift passing from B3LYP to MP2 geometries. A significantly larger increase is obtained for the CHINO system while a reduction is found for the ACRI system.

Let us try to rationalize these observations using the neutral/zwitterionic picture presented in the introduction and reported in Figure 1.

When the solvent polarity increases we expect that the ground state becomes more zwitterionic and BLA more and more negative. The excited state is also stabilized in polar solvents but not as much as the ground state and a solvatochromic blue shift is found. This model seems to apply to the PYRI system whatever is the geometry used. In that system in fact, the ground state is essentially zwitterionic (as discussed in the previous section) at both B3LYP and MP2 level. As a result the electronic transition can be viewed as a charge transfer from the negatively charged dicyano group to the N-alkylazinium group.

By contrast, in the ACRI system, we have seen that the MP2 ground state has a more neutral character and a less important solvent dependency than the B3LYP one. In this case the flow of electronic charge on excitation seems to have an opposite direction with respect to what found in the PYRI system, from the aminoquinoid group to the dicyano group. As a result, the corresponding excited state has a prevalent zwitterionic character that is similar in all solvents and the solvatochromic shift becomes smaller.

In general, MP2 geometries (when used in combination with TDCAMB3LYP) seem to give the most accurate description of the absorption process in the three systems. To check if this behavior is due to a fortuitous combination due to the relatively small basis set we used, a test with larger basis sets (6-311+G(d) and 6-311++G(d,p)) has been done on the PYRI system. The differences obtained on the transition energies are less than 1% with all solvents and the signs of the shifts passing from one solvent to the other do not change with respect to the results obtained with the smaller basis set.

A further analysis that can be used to rationalize structure and solvent effects on the electronic nature of ground and excited state can be obtained in terms of atomic populations. In Figure 4, we report the variation of the Merz−Kollman (MK)[39] charges passing from ground to excited states for the PYRI and the ACRI system. In particular, we have plotted the change in the MK charges of the two terminal groups passing from ground to excited states. All data refer to (TD)CAMB3LYP calculations with MP2 geometries.

Concerning the ground state, the PYRI system presents the typical charge distribution of the zwitterionic form as predicted from the previous analysis on BLA, a large and negative value on the dicyano residue and a large positive value on pyridinic residue (especially in polar solvents). In the ACRI system, the dicyano residue has a much smaller charge, and in parallel the acridinic residue becomes much less positive (in agreement with the BLA positive value discussed in the previous section). If now we consider the excited state, we see that in the PYRI system the charge on dicyano residue is still negative but smaller

in magnitude with respect to the ground state thus showing a less zwitterionic character for such a state due to a charge flow to the pyridinic group. By contrast, in the ACRI system the dicyano charge becomes more negative and the acridinic charge becomes significantly positive. This opposite behaviors is clearly shown in Figure 4 in which an opposite charge flow seems to be associated with the two systems (namely from the dicyano group to the pyridinic group in the PYRI system and from the ACRI to the dicyano residue in the ACRI system). In addition, the two systems present a further opposite behavior, the charge flow (either in one or in the opposite direction) becomes more efficient in polar solvents for PYRI system and in apolar solvents for the ACRI systems. This trend exactly follows the parallel one on solvatochromic shifts (blue and decreasing with polarity for the PYRI system and red and increasing with solvent polarity). The explanation is easily given in terms of the preferential stabilization that polar solvents have on more zwitterionic systems which, for PYRI is the ground state and for ACRI is the excited state.

3.4. Hyperpolarizability. In the previous section, we analyzed in detail both ground- and excited-state properties of the three systems in different solvents; now, we move to present and discuss the related NLO properties. In this section, two different estimates of the static hyperpolarizability will be considered, namely, that obtained assuming a TLM and that obtained as FF difference of analytic polarizabilities.

3.4.1. A Comparison with Experiments. Within the TLM approximation, it is possible to obtain experimental estimates of the static hyperpolarizability (β_0) using the electro-optical absorption (EOA) approach.[5,40] This is a powerful experimental technique that can be used for characterizing the CT band of a push−pull molecule. In an EOA experiment, one measures the effect of an externally applied electric field on the molar decadic absorption coefficient, and from such a measurement the ground-state dipole moment and the ground-to-excited dipole difference $\Delta\mu$ can be calculated. By using EOA data together with experimental excitation energies (ΔE) and transition dipole moments (μ^T), the static hyperpolarizability can be estimated within the TLM approximation as

$$\beta_0 = \frac{6\Delta\mu(\mu^T)^2}{\Delta E^2} \quad (1)$$

where the Taylor convention has been used for both the sign and prefactors.[48] This equation can be obtained from the full sum-over-state (SOS) expression by reducing the sum to only one excited state (the CT state) and assuming that one tensorial component dominates the response (i.e., the charge-transfer is unidirectional). We note that in all the three systems studied there is an (almost) axial symmetry, and the dipole moments (including the transition ones) are dominated by the x component where x is the axis connecting the central carbon in the cyano group with the nitrogen of the azinium group. The differences obtained in the estimate of β_0 when using the x components only or the full vectors are less than 1%.

Owing to the strong electric field required for EOA measurements, spectra are recordable only in solvents with low dielectric constants to avoid dielectric breakdown. This is the reason why experimental data are available only in dioxane solution as reported in Table 2.

In Table 3, a study on the influence of the QM description on TLM hyperpolarizabilities of the three investigated systems in dioxane is reported. TDB3LYP and TDCAM-B3LYP descriptions have been used for both B3LYP and MP2 geometries.

TABLE 2: EOA Data in Dioxane[10a]

	PYRI	CHINO	ACRI
μ_{GS}	20.0	16.9	9.8
μ_{EX}	17.3	18.5	23.8
$\Delta\mu$	−2.7	1.6	14.0
μ^T	11.1	11.1	9.5
β_0	−254 ± 40	175 ± 48	762[41] ± 38

[a] Dipole moments are in Debye and hyperpolarizabilities in 10^{-30} esu.

TABLE 3: TDDFT Results for the Three Investigated Systems in Dioxane Using Two Different Sets of Geometries (B3LYP and MP2); Dipole Moments Are in Debye and Hyperpolarizability Values Are in 10^{-30} esu

	TDB3LYP		TDCAMB3LYP	
geom	B3LYP	MP2	B3LYP	MP2
		PYRI		
μ_{GS}	27.4	27.2	28.6	28.2
μ_{EX}	26.2	26.0	27.5	27.4
$\Delta\mu$	−1.3	−1.2	−1.0	−0.8
μ^T	14.1	14.0	14.5	14.4
β_0	−123	−112	−105	−87
		CHINO		
μ_{GS}	25.4	25.0	24.7	25.5
μ_{EX}	23.7	23.9	25.7	25.8
$\Delta\mu$	−1.7	−1.1	1.0	0.3
μ^T	14.4	14.4	14.7	14.8
β_0	−187	−129	109	35
		ACRI		
μ_{GS}	19.9	18.6	19.6	18.1
μ_{EX}	22.5	23.1	23.7	23.5
$\Delta\mu$	2.6	4.6	4.1	5.4
μ^T	13.0	12.6	13.9	13.3
β_0	270	400	399	454

By comparing with the experimental results reported in Table 2, it is evident that the best description is obtained with TDCAM-B3LYP. A comparison of these results with EOA data leads to a generalized and satisfactory agreement, showing that TDCAM-B3LYP gives a good description of the excited state as already suggested by the previous analysis on the absorption energies.

Moving to a more detailed comparison with experiments, we see that dipole moment changes from the ground state to the first excited state are generally underestimated, though sign and trend are correctly reproduced when TDCAMB3LYP is used. At TDB3LYP level, the sign of the calculated $\Delta\mu$ is correct for PYRI and ACRI systems but not for CHINO. As the sign of $\Delta\mu$ determines the sign of β_0, also for the latter TDCAMB3LYP represents the best description. Calculated transition dipole moments are generally larger than experimental ones, however the trend passing one system to the other is correctly reproduced, with PYRI and CHINO μ^T being very similar and larger than in ACRI system.

If we now analyze the effect of the different geometry, we see that changes increase passing from PYRI to CHINO and to ACRI, which presents the largest sensitivity (for example the dipole moment of the ground state changes of ca. 1.5 D at both B3LYP and CAMB3LYP level). This is perfectly explained by the BLA values reported in Figure 2.

From the global comparison of Tables 2 and 3 (together with data reported in Table 1) we can conclude that the most accurate level of calculation is represented by TDCAM-B3LYP at MP2 geometries. This combination in fact correctly reproduces experimental trends both in absorption energies and in response

TABLE 4: TLM TD-CAMB3LYP Hyperpolarizabilities (10^{-30} esu) for the Three Investigated Systems in Gas-Phase and in Different Solvents[a]

	PYRI	CHINO	ACRI
gas	64	90	234
dioxane	−87	35	454
$CHCl_3$	−760	−438	721
DMSO	−1256	−1782	1029

[a] In all cases MP2 geometries have been used.

TABLE 5: FF CAMB3LYP Hyperpolarizabilities (10^{-30} esu) for the Three Investigated Systems in Gas-Phase and in Different Solvents[a]

	PYRI		CHINO		ACRI	
	β_{xxx}	β_x	β_{xxx}	β_x	β_{xxx}	β_x
gas	4	−1	26	−32	−86	−95
dioxane	179	165	74	56	−196	−218
$CHCl_3$	708	685				
DMSO	1013	985	1375	1346	−439	−499

[a] In all cases MP2 geometries have been used.

properties. Therefore, in the following analysis B3LYP will not be further used.

3.4.2. Interplay of Solvent and Structural Effects. In the previous section, we have analyzed TDDFT estimates of β in dioxane using a TLM approximation. Here, a study of the solvent effects is presented by comparing TLM and FF estimates of the same response property.

In the TLM approximation, we have assumed that the general SOS expression determining the static β can be reduced to two states only; within the FF approach, by contrast, the explicit determination of the excited states is not required. In the present study, FF values of β are obtained as finite differences of analytic polarizabilities (the standard two-point finite dipole difference formulas is used[47]). The polarizabilities are obtained in an analytical way by using a coupled perturbed SCF approach.[25] The same approach has been also extended to multiconfigurational SCF,[42] perturbative approaches such as MP2,[43] coupled cluster,[44] and DFT.[45] More recently, it has been coupled to IEFPCM to account for solvent effects.[46]

In all of the three systems studied, there is an (almost) axial symmetry; as a result, the β tensor will be dominated by the β_{xxx} component. In the experiments, however, combinations of different components are often used; for the studied system, the commonly used one is[48]

$$\beta_x = \frac{1}{3}\sum_j (\beta_{xjj} + \beta_{jxj} + \beta_{jjx}) \quad (j = x, y, z) \qquad (2)$$

In Table 4 and 5 we report TLM and FF values of β obtained for the three systems in the various solvents at (TD)CAMB3LYP/6-31+G(d) level using MP2 geometries. To have a more complete analysis of the changes induced by the tuning of the environment properties, gas-phase data are also reported.

We have to recall that in order to have a correct comparison between FF and TLM estimates, we have to distinguish between the apolar (dioxane) and the polar solvents. The FF values of static β in fact are obtained assuming a complete response of the solvent while the standard way to get transition energies and dipole moments is using a nonequilibrium solvation regime. In the nonequilibrium regime, the solvent responds with its electronic (or optical) permittivity while the equilibrium solvation is determined by the full (static) permittivity (which also includes the orientational or inertial part of the dielectric response). For apolar solvents, static and optical permittivities coincide (i.e., there is no orientational contribution) but for polar solvents they are very different, for example for DMSO $\epsilon(0) = 46.7$ while $\epsilon_{opt} = 2.18$. Because of these different solvation regimes, to have a TLM estimate that can be compared with the FF values also for polar solvents we have to recompute both transition energies and dipole moments assuming a complete (equilibrium) response of the solvent. The results obtained within such a framework are reported in Table 4 where we also repeat the results for dioxane already reported in Table 3.

TABLE 6: FF MP2 Hyperpolarizabilities (10^{-30} esu) for the Three Investigated Systems in Gas-Phase and in Different Solvents[a]

	PYRI		CHINO		ACRI	
	β_{xxx}	β_x	β_{xxx}	β_x	β_{xxx}	β_x
gas	−250	−257	−257	−241	−241	−253
Dioxane	−69	−86	−469	−495	−511	−536
$CHCl_3$	1368	1345				
DMSO	1555	1536	2117	2098	−1144	−1209

[a] In all cases MP2 geometries have been used.

The TLM results reported in Table 4 can be related to the BLA values reported in the previous section. For PYRI and CHINO systems, a crossing of the cyanine limit in low polar solvents (close to dioxane for PYRI system and close to $CHCl_3$ for CHINO system) was found. We recall that in this limit the system has the maximum level of conjugation and hyperpolarizability β becomes zero. This is confirmed by the TDCAMB3LYP β values that change sign passing from gas-phase to dioxane in PYRI system and from dioxane to $CHCl_3$ in CHINO system. By contrast, for ACRI system β remains positive in all environments (including gas-phase) and it increases with solvent polarity. Once again, this behavior is coherent with what found for BLA which is always positive for ACRI system (i.e., the system is always in the neutral form).

Comparing the values reported in Table 4 and 5, it is evident that the two different descriptions of β lead to very different qualitative and quantitative behaviors. To confirm such a behavior, we have repeated both TLM and FF calculations using two larger basis sets (those already tested for UV/vis results, namely 6-311+G(d) and 6-311++G(d,p)); this test has been limited to PYRI in the two opposite solvents (dioxane and DMSO). The behavior found with 6-31+G(d) is completely confirmed using the two larger basis sets; the variations found on β are of ca. 10 and 8% for dioxane and ca. 2 and 1% for DMSO at FF or TLM level of calculation, respectively.

To have a further check on the reliability of CAMB3LYP to describe hyperpolarizabilities, we have repeated FF calculations for the three systems in the different environments at MP2/6-31G(d) level. The obtained β values are reported in Table 6.

Even if the absolute values of β differ with respect to FF-CAMB3LYP ones, FF-MP2 results confirm the same qualitative behaviors. β_{xxx} changes sign for PYRI and CHINO becoming large and positive in polar solvents while it is always negative for ACRI (increasing in module with solvent polarity). This gives a further support to the reliability of the FF-DFT results and it confirms the differences with respect to the TLM description. To investigate possible sources of these differences, we have compared the analytical polarizabilities used to obtain β with the TLM estimate defined as

$$\alpha_0^{\mathrm{TLM}} = \frac{2(\mu^{\mathrm{T}})^2}{\Delta E} \quad (3)$$

As for the analysis on β also here, for polar solvents we have to introduce an equilibrium solvation when calculating the quantities required in the definition of α_0^{TLM}. The results are reported in Table 7.

TLM and analytical polarizabilities present the same trend with the solvent polarity but different absolute values. The TLM approximation accounts for 60−70% of the analytical value in gas phase and in solution. This result is an indication that contributions due to higher excited states are important already at the polarizability level. These missing terms evidently become much more important passing to β. The analysis of the contributions of higher excited states is however much more complicated in that property as such contributions can be either positive or negative (depending on the sign of $\Delta\mu$) while for α only positive terms are possible.

Still on the results of Table 6, we note that the agreement of TDCAMB3LYP α_0^{TLM} with experimental TLM estimates in dioxane is very good in terms of the expected changes passing from one system to the other but calculated values are always larger. This can be explained in terms of possible inaccuracies of TDCAMB3LYP to describe both absorption energies and transition dipoles (see also Tables 1−3).

To better analyze the discrepancy between TLM and FF results, it is better to recall the SOS estimate of α and β; namely, using the representation by Orr and Ward,[49] we have

$$\alpha_0^{\mathrm{SOS}} = \sum_{j\neq 0} \frac{2(\mu_{0j}^{\mathrm{T}})^2}{\Delta E_{0j}}; \quad \beta_0^{SOS} = \sum_{j\neq 0} \frac{6\Delta\mu_{0j}(\mu_{0j}^{\mathrm{T}})^2}{\Delta E_{0j}^2} + \sum_{j\neq 0}\sum_{k\neq l\neq 0} \frac{6\mu_{0j}^{\mathrm{T}}\mu_{jk}^{\mathrm{T}}\mu_{ko}^{\mathrm{T}}}{\Delta E_{0j}\Delta E_{0k}} \quad (4)$$

where we have assumed that only the diagonal component along the molecular axis (here x) is significative. To obtain the SOS estimate of β, transition dipoles between excited states are necessary. Within the Gaussian computational code (version G03), these quantities are not available at TDDFT level but they can be obtained in the CIS approximation. Still remaining in this approximation, expensive calculations should be performed to obtain not only the excitation energies and the corresponding transition dipoles but also the variation of the dipole moment. To reduce such an amount of calculations, we have limited the analysis to the changes induced on the TLM estimate of β_0^{SOS} by the second term of eq 4 still in the approximation that $j = 1$. The SOS-CIS results obtained for the PYRI system in different environments are reported in Table 8 together with the corresponding TLM-CIS estimates and the analytical HF values.

Looking first at the comparison between TLM and analytical values, we note that the discrepancies found at (TD)CAMB3LYP level are confirmed also at HF/CIS level. This is further indirect proof that what found is not dependent on the QM level of calculation. Let us now move to analyze the higher-states contribution.

For polarizability for which any truncated SOS estimate necessarily underestimates the analytical value (all terms in the SOS expression are in fact positive), we observe that extending the sum to 100 excited states does not lead to a converged value, but only to an increase of about 10 (gas phase) to 8% (DMSO) with respect to the TLM value. The analysis becomes much more intricate when hyperpolarizability is considered. For this property in fact, different terms in the SOS expression can have different sign. In gas phase, the contribution from the second term is opposite in sign with respect to the TLM term; as a result the β value is significantly reduced. On the contrary, in dioxane the two contributions (with same sign) sum up in a final large and negative SOS value. Finally, for DMSO, the contribution from the second term is small with respect to the TLM estimate and β_0^{SOS} does not significantly change with respect to β_0^{TLM} value. These very different behaviors with the different environments are clearly of limited use as $j > 1$ terms should also be included. However, they are a clear proof of the difficulty of the analysis of the evolution of the NLO response with the number of excited states. In the literature only a few ab initio studies have explicitly looked at this aspect.[2,51]

TABLE 7: Analytic and TLM Polarizabilities Obtained at (TD)CAMB3LYP level for the Three Investigated Systems in Gas-Phase and in Different Solvents[a]

	α_{xx}	α_0^{TLM}	α_0^{TLM}(exp)
		PYRI	
gas	134	95 (70)	
Dioxane	175	131 (75)	98
$CHCl_3$	191	150 (79)	
DMSO	167	124 (74)	
		CHINO	
gas	151	105 (73)	
Dioxane	199	145 (73)	105
DMSO	204	149 (73)	
		ACRI	
gas	135	80 (60)	
Dioxane	172	110 (64)	64
DMSO	237	173 (73)	

[a] In parentheses we report the percent TLM estimate with respect to the analytical ones. In all calculations, MP2 geometries have been used. For the TLM estimates, experimentally derived values are also reported.[10] All values are in 10^{-40} C V^{-1} m^2.

As a final analysis, we report the trends with respect to different solvents and structural changes of a quantity which is generally used to quantify the potentiality of a chromophore to act as an efficient NLO probe. This quantity is defined as

$$\mu\cdot\beta = \sum_j \mu_j\beta_j \quad (j = x, y, z) \quad (5)$$

This last analysis allows also a more direct comparison with the computational results reported in the reference paper by Abbotto et al. These latter refer to HF/6-31G(d) calculations on HF/6-31G(d) geometries (imposing C_s symmetry for all systems); solvent effects have been taken into account using the Onsager solvation model.

TABLE 8: TLM, SOS, and Analytical (Hyper)Polarizabilities Obtained at CIS/6-31+G(d) and HF/6-31+G(d) Level for PYRI System in Gas-Phase and in Different Solvents[a]

	α_0^{TLM}	α_0^{SOS}	α_{xx}	β_0^{TLM}	β_0^{SOS}	β_{xxx}
gas	92(71)	104(81)	129	111	48	33
Dioxane	107(66)	120(73)	163	−41	−97	260
DMSO	74(56)	89(68)	131	−493	−493	590

[a] In parentheses we report the percent estimate with respect to the analytical ones. In all calculations, MP2 geometries have been used. α values are in 10^{-40} C V^{-1} m^2 and β in 10^{-30} esu.

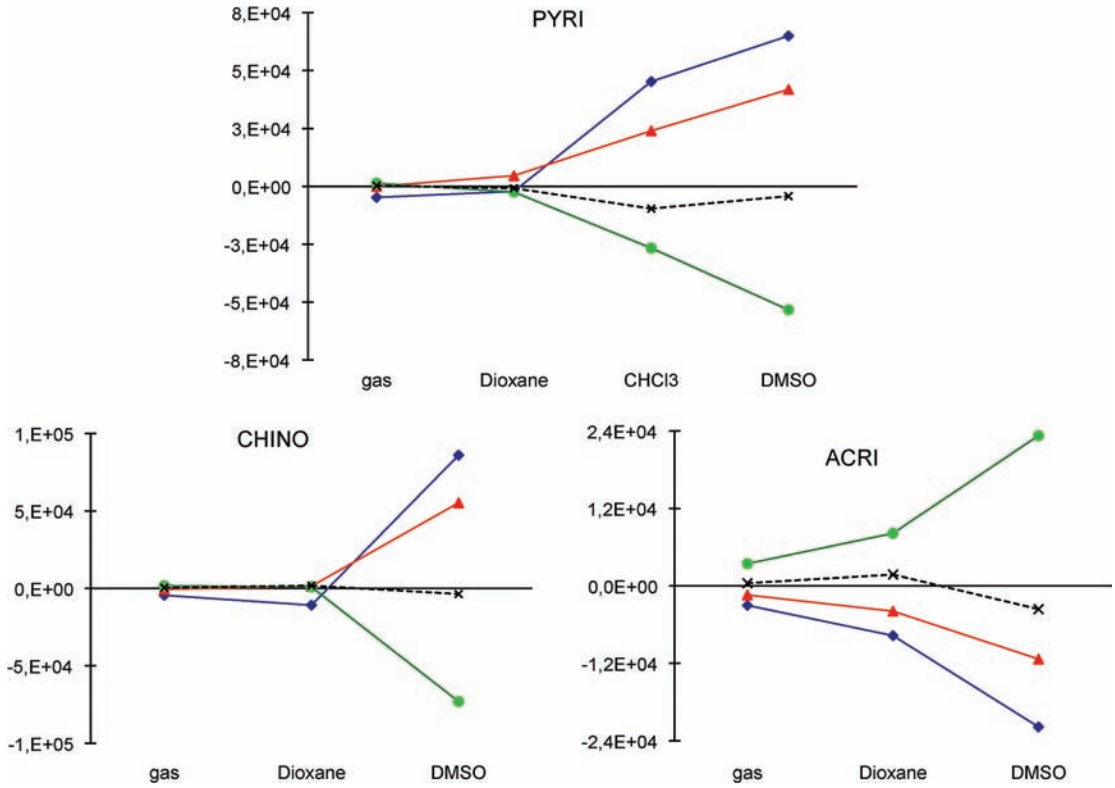

Figure 5. FF CAMB3LYP (red), FF MP2 (blue), and TLM (green) $\mu \cdot \beta$ values for three different systems with respect to different environments. Points connected with dotted lines refer to HF/6-31G(d) calculations using the Onsager solvation model as reported in ref 10 (values indicated as DMSO actually refer to DMF). All values are in 10^{-48} esu.

The results obtained for the three systems are reported in Figure 5.

As expected from the previous analysis, we observe that FF-CAMB3LYP and FF-MP2 give quite similar behaviors that strongly differ from TLM. The older calculations show a by far lower sensitiveness to the solvent than the present ones. This can be explained in terms of the different solvation model used; in the reference paper in fact, the Onsager model was used to include solvent effects. In a such a model, the solute is assumed to be contained in a spherical cavity of radius derived from the real molecular volume and the solute charge distribution is approximated to a dipole. These different approximations (and in particular the first one on the cavity) are the source of the differences found with respect to PCM data. In particular, the use of the spherical cavity necessarily induces a smaller solvent effect both in the geometry optimization and in the calculation of the response properties. The two effects when combined are reflected in the very flat curves of $\mu \cdot \beta$ with respect to the solvent.

The graphs reported in Figure 5 better clarify the interplay between solvent and structural (i.e., annelation) effects, which we summarize as follows:

(i) In gas phase, all the systems are characterized by a molecular structure frozen in the neutral (quinoid) limit formula. At this limit condition, annelation of the pyridine acceptor has not large influence on the extent of the charge transfer and on the molecular property.

(ii) In media possessing low dielectric constants (dioxane), the description of the dyes' ground or excited states becomes a combination of both quinoid and zwitterionic limit formulas, which can easily be perturbed. In this situation, structural modifications largely affect the nonlinear optical response. In particular, we observe a depletion of the NLO activity passing from PYRI to CHINO system.

(iii) In highly polar solvents, PYRI and CHINO have a dominant contribution of the zwitterion form while in ACRI the neutral form is still predominant. This is reflected in the graph in which $\mu \cdot \beta$ changes sign passing from CHINO to ACRI.

These graphs confirm what was suggested in the experimental characterization of the systems, namely, that the NLO performance not only relies on a proper choice of structural components but varies by orders of magnitude as a function of the medium polarity. In particular, only an appropriate combination of molecular design and of solvent leads to an excellent NLO activity while by changing only one of these two parameters the same NLO response can completely vanish.

To conclude, it is important to note that this delicate interplay between solvent and structure is similarly described by FF and TLM descriptions even if with almost specular behaviors. This is indeed a remarkable result; in fact, the SOS analysis has clearly shown that TLM cannot give correct NLO properties although the results reported in Figure 5 show that TLM reproduces the FF trends of $| \mu \cdot \beta |$ in the various solvents.

4. Final remarks

We have presented a quantum mechanical study of a class of highly polarizable merocyanine compounds belonging to the family of azinium-(CH═CH-thyenil)-dicyanomethanido chromophores in different solvents. In this class of chromophores, the response properties are strongly affected by the modulation of the charge transfer through consecutive annelation of the pyridyl ring. This annelation effect can in fact cause significant bond alternation and influence the relative importance of the

aromatic/quinoid character of the azinium ring. A combined study of electronic excitations, NMR and (hyper)polarizabilities is used to rationalize the cooperative interplay of solvent and structural changes in determining the potential second-order NLO activity of these push−pull compounds.

The three systems studied have shown very different structural and electronic properties that are finally reflected in the related behaviors of the (hyper)polarizabilities with solvent; each system has shown to present the optimal NLO response in an environment that is specific for it but not necessarily for the others. A careful quantum-mechanical description is thus necessary to correctly predict these behaviors; correlated DFT approaches are possible effective strategies but only when accurately checked with respect to more stable formulations such as MP2. In addition, a coupling of correlated methods with solvation models that can properly account for geometrical and electronic changes among the systems is of fundamental importance. The PCM approach used here, even if limited to a continuum picture of the solvent, can represent a possible choice. The use of a detailed cavity that follows the real geometrical structure of the solute and the use of a response operator determined by the full QM charge distribution of the solute introduces a more accurate description of the solvent response with respect to other, widely used solvation models either based on a simplified cavity or a simplified description of the solute charge distribution.

Finally, a critical analysis of the approximation commonly used to predict NLO activities has been performed by comparing FF values of α and β with their estimates obtained adopting the two-level model. The comparison clearly shows strong limitations of the simplified TLM description in quantitatively reproducing the NLO properties. However, the same comparison also confirms TLM as a useful tool in supporting and interpreting qualitative trends in the nonlinear response with environmental and structural changes.

References and Notes

(1) (a) Prasad, P. N.; Williams, D. J. *Introduction to Nonlinear Optical Effects in Molecules and Polymers*; Wiley: New York, 1991. (b) Chemla, D. S.; Zyss, J. *Nonlinear Optical Properties of Organic Molecules and Crystals*; Academic Press: New York, 1987. (c) Nalwa, H. S.; Miyata, S. *Nonlinear Optics of Organic Molecules and Polymers*; CRC Press: Boca Raton, FL, 1997.

(2) Kanis, D. R.; Ratner, M. A.; Marks, T. J. *Chem. Rev.* **1994**, *94*, 195.

(3) Bishop, D. M. *Adv. Chem. Phys.* **1998**, *104*, 1.

(4) (a) Marder, S. R.; Kippelen, B.; Jen, A. K.-Y.; Peyghambarian, N. *Nature* **1997**, *388*, 845. (b) Marder, S. R.; Cheng, L. T.; Tiemann, B. G.; Friedli, A. C.; Blanchard-Desce, M.; Perry, J. W.; Skindhoej, J. *Science* **1994**, *263*, 511. (c) Marder, S. R.; Gorman, C. B.; Tiemann, B. G.; Cheng, L. T. *J. Am. Chem. Soc.* **1993**, *115*, 2524. (d) Marder, S. R.; Beratan, D. N.; Cheng, L.-T. *Science* **1991**, *252*, 103.

(5) Wolff, J. J.; Wortmann, R. *Adv. Phys. Org. Chem.* **1999**, *32*, 121.

(6) (a) Oudar, J. L. *J. Chem. Phys.* **1977**, *67*, 446. (b) Oudar, J. L.; Chemla, D. S. *J. Chem. Phys.* **1977**, *66*, 2664.

(7) (a) Barzoukas, M.; Blanchard-Desce, M.; Josse, D.; Lehn, J.-M.; Zyss, *J. Chem. Phys.* **1989**, *133*, 323. (b) Stähelin, M.; Burland, D. M.; Rice, J. E. *Chem. Phys. Lett.* **1992**, *191*, 245. (c) Zyss, J.; Ledoux, I. *Chem. Rev.* **1994**, *77*, 94. (d) Painelli, A.; Terenziani, F. *Chem. Phys. Lett.* **1999**, *312*, 211.

(8) (a) Wortmann, R.; Kramer, P.; Glania, C.; Lebus, S.; Detzer, N. *Chem. Phys.* **1993**, *173*, 99. (b) Wortmann, R.; Poga, C.; Twieg, R. J.; Geletneky, C.; Moylan, C. R.; Lundquist, P. M.; DeVoe, R. G.; Cotts, P. M.; Horn, H.; Rice, J. E.; Burland, D. M. *J. Chem. Phys.* **1996**, *10637*, 105. (c) Blanchard-Desce, M.; Alain, V.; Bedworth, P. V.; Marder, S. R.; Fort, A.; Runser, C.; Barzoukas, M.; Lebus, S.; Wortmann, R. *Chem.—Eur. J.* **1997**, *3*, 1091.

(9) Bartkowiak, W.; Zaleśny, R. SOS Methods in Calculations of Electronic NLO Properties. In *Non-Linear Optical Properties of Matter*; Papadopoulos, M. G., Sadlej, A. J., Leszczynski, J., Eds.; Springer: Netherlands, 2006; Vol. 1, p 129.

(10) (a) Abbotto, A.; Beverina, L.; Bradamante, S.; Facchetti, A.; Klein, C.; Pagani, G. A.; Abshiro, M. R.; Wortmann, R. D. *Chem.—Eur. J.* **2003**, *9*, 1991. (b) Archetti, G; Abbotto, A.; Wortmann, R. D. *Chem.—Eur. J.* **2006**, *12*, 7151.

(11) See, for example, the two reviews:(a) Olsen, J.; Jørgensen, P. In *Modern Electronic Structure Theory*; Yarkony, D. R., Ed.; World Scientific: Singapore, 1995; Vol. 2, p 857;(b) Luo, Y.; Ågren, H.; Mikkelsen, K. V.; Jørgensen, P. *Adv. Quantum Chem.* **1995**, *26*, 165.

(12) Shelton, D. P.; Rice, J. E. *Chem. Rev.* **1994**, *94*, 3.

(13) (a) Champagne, B.; Perpete, E. A.; van Gisbergen, S. J. A.; Baerends, E. J.; Snijders, J. G.; Soubra-Ghaoui, C.; Robins, K. A.; Kirtman, B. *J. Chem. Phys.* **1998**, *109*, 10489. (b) Champagne, B.; Perpete, E. A.; Jacquemin, D.; van Gisbergen, S. J. A.; Baerends, E. J.; Soubra-Ghaoui, C.; Robins, K. A.; Kirtman, B. *J. Phys. Chem. A* **2000**, *104*, 4755.

(14) Gruning, M.; Gritsenko, O. V.; van Gisbergen, S. J. A.; Baerends, E. J. *J. Chem. Phys.* **2002**, *116*, 9591.

(15) Tomasi, J.; Mennucci, B.; Cammi, R. *Chem. Rev.* **2005**, *105*, 2999.

(16) *Continuum solvation models in chemical physics, from teory to applications*; Mennucci, B.; Cammi, R., Eds.; Wiley: Chichester, 2007.

(17) Wortmann, R.; Bishop, D. M. *J. Chem. Phys.* **1998**, *108*, 1001.

(18) (a) Luo, Y.; Norman, P.; Ågren, H. *J. Chem. Phys.* **1998**, *13*, 21. (b) Norman, P.; Macak, P.; Luo, Y.; Ågren, H. *J. Chem. Phys.* **1999**, *110*, 7960. (c) Macak, P.; Norman, P.; Luo, Y.; Ågren, H. *J. Chem. Phys.* **2000**, *112*, 1868.

(19) Willetts, A.; Rice, J. E. *J. Chem. Phys.* **1993**, *99*, 426.

(20) Yu, J.; Zerner, M. C. *J. Chem. Phys.* **1994**, *100*, 7487.

(21) (a) Mikkelsen, K. V.; Jørgensen, P.; Jensen, H. J. Aa. *J. Chem. Phys.* **1994**, *100*, 6597. (b) Mikkelsen, K. V.; Sylvester-Hvid, K. O. *J. Phys. Chem.* **1996**, *100*, 9116. (c) Sylvester-Hvid, K. O.; Mikkelsen, K. V.; Jonsson, D.; Norman, P.; Ågren, H. *J. Chem. Phys.* **1998**, *5576*, 109. (d) Sylvester-Hvid, K. O.; Mikkelsen, K. V.; Jonsson, D.; Norman, P.; Ågren, H. *J. Phys. Chem. A* **1999**, *103*, 8375. (e) Christiansen, O.; Mikkelsen, K. V. *J. Chem. Phys.* **1999**, *110*, 8348. (f) Sylvester-Hvid, K. O.; Mikkelsen, K. V.; Norman, P.; Jonsson, D.; Ågren, H. *J. Phys. Chem. A* **2004**, *108*, 8961.

(22) Miertus, S.; Scrocco, E.; Tomasi, J. *Chem. Phys.* **1981**, *55*, 117.

(23) (a) Cancès, E.; Mennucci, B. *J. Math. Chem.* **1998**, *23*, 309. (b) Cancès, E.; Mennucci, B.; Tomasi, J. *J. Chem. Phys.* **1997**, *107*, 3032. (c) Mennucci, B.; Cancès, E.; Tomasi, J. *J. Phys. Chem. B* **1997**, *101*, 10506.

(24) (a) Cammi, R.; Cossi, M.; Mennucci, B.; Tomasi, J. *Chem. Phys.* **1996**, *105*, 10556. (b) Cammi, R.; Mennucci, B.; Tomasi, J. *J. Phys. Chem. A* **1998**, *102*, 870. (c) Cammi, R.; Mennucci, B.; Tomasi, J. *J. Phys. Chem. A* **2000**, *104*, 4690. (d) Cammi, R.; Mennucci, B.; Tomasi, J. In *Nonlinear Optical Responses of Molecules Solids and Liquids: Methods and Applications*; Papadopoulos, M. G., Ed.; Research Signpost: Kerala, 2003; p 113.

(25) (a) Dykstra, C. E.; Jasien, P. G. *Chem. Phys. Lett.* **1984**, *109*, 388. (b) Olsen, J.; Jørgensen, P. *J. Chem. Phys.* **1985**, *82*, 3235. (c) Sekino, H.; Bartlett, R. J. *J. Chem. Phys.* **1986**, *85*, 976. (d) Karna, S. P.; Dupuis, M. *J. Comput. Chem.* **1991**, *12*, 487. (e) Rice, J. E.; Handy, N. C. *Int. J. Quantum Chem.* **1992**, *43*, 91.

(26) Jacquemin, D.; Femenias, A.; Chermette, H.; Ciofini, I.; Adamo, C.; Andre, J.-M.; Perpete, E. A. *J. Phys. Chem. A* **2006**, *110*, 5952.

(27) (a) Becke, A. D. *Phys. Rev. A* **1988**, *38*, 3098. (b) Lee, C. T.; Yang, W. T.; Parr, R. G. *Phys. Rev. B* **1988**, *37*, 785.

(28) (a) Casida, M. E. In *Recent Advances in Density Functional Methods*; Chong, D. P., Ed.; World Scientific: Singapore, 1995; (b) Gross, E. U. K.; Dobson, J. F.; Petersilka, M. In *Density Functional Theory II*; Nalewajski, R. F., Ed.; Springer: Heidelberg, 1996. (c) Bauernschmitt, R.; Ahlrichs, R. *Chem. Phys. Lett.* **1996**, *256*, 454. (d) Stratmann, R. E.; Scuseria, G. E.; Frisch, M. J. *J. Chem. Phys.* **1998**, *109*, 8218. (e) Hirata, S.; Head-Gordon, M. *Chem. Phys. Lett.* **1999**, *314*, 291.

(29) (a) Tozer, D. J.; Amos, R. D.; Handy, N. C.; Roos, B. J.; Serrano-Andres, L. *Mol. Phys.* **1999**, *97*, 859. (b) Cai, Z.-L.; Sendt, K.; Reimers, J. R. *J. Chem. Phys.* **2002**, *117*, 5543. (c) Grimme, S.; Parac, M. *Chem. Phys. Chem.* **2003**, *3*, 292. (d) Dreuw, A.; Weisman, J. L.; Head-Gordon, M. *J. Chem. Phys.* **2003**, *119*, 2943. (e) Peach, M. J. G.; Benfield, P.; Helgaker, T.; Tozer, D. J. *J. Chem. Phys.* **2008**, *128*, 044118.

(30) (a) Leininger, T.; Stoll, H.; Werner, H.-J.; Savin, A. *Chem. Phys. Lett.* **1997**, *275*, 151. (b) Iikura, H.; Tsuneda, T.; Yanai, T.; Hirao, K. *J. Chem. Phys.* **2001**, *115*, 3540. (c) Vydrov, O. A.; Heyd, J.; Krukau, A. V.; Scuseria, G. E. *J. Chem. Phys.* **2006**, *125*, 074106.

(31) Yanai, T.; Tew, D. P.; Handy, N. C. *Chem. Phys. Lett.* **2004**, *393*, 51.

(32) (a) Ferrighi, L.; Frediani, L.; Cappelli, C.; Sałek, P.; Ågren, H.; Helgaker, T.; Ruud, K. *Chem. Phys. Lett.* **2006**, *425*, 267. (b) Peach, M. J. G.; Helgaker, T.; Sałek, P.; Keal, T. W.; Lutnaes, O. B.; Tozer, D. J.; Handy, N. C. *Phys. Chem. Chem. Phys.* **2006**, *8*, 558. (c) Jacquemin, D.; Perpete, E. A.; Scalmani, G.; Frisch, M. J.; Kobayashi, R.; Adamo, C. *J. Chem. Phys.* **2007**, *126*, 144105. (d) Jacquemin, D.; Perpete, E; Medved, M.; Scalmani, G.; Frisch, M. J.; Kobayashi, R.; Adamo, C. *J. Chem. Phys.* **2007**, *126*, 191108.

(33) Rappe, A. K.; Casewit, C. J.; Colwell, K. S.; Goddard, W. A.; Skiff, W. M. *J. Am. Chem. Soc.* **1992**, *114*, 10024.

(34) Frisch, M. J. et al.; *Gaussian Development Version*; Gaussian, Inc.: Wallingford, CT, 2008.

(35) (a) Hameka, H. F. *Rev. Mod. Phys.* **1962**, *34*, 87. (b) Ditchfield, R. *Mol. Phys.* **1974**, *27*, 789. (c) Wolinski, K.; Hinton, J. F.; Pulay, P. *J. Am. Chem. Soc.* **1990**, *112*, 8251.

(36) (a) Van Caillie, C.; Amos, R. D. *Chem. Phys. Lett.* **1999**, *308*, 249. (b) Furche, F.; Ahlrichs, R. *J. Chem. Phys.* **2004**, *117*, 7433.

(37) Frediani, L.; Rinkevicius, Z; Ågren, H. *J. Chem. Phys.* **2005**, *122*, 244104.

(38) Scalmani, G.; Frisch, M. J.; Mennucci, B.; Tomasi, J.; Cammi, R.; Barone, V. *J. Chem. Phys.* **2006**, *124*, 094107.

(39) Besler, B. H.; Merz, K. M., Jr.; Kollman, P. A. *J. Comput. Chem.* **1990**, *11*, 431.

(40) (a) Liptay, W. Dipole Moments and Polarizabilities of Molecules in Excited Electronic States. In *Excited States*; Lim, E. C., Ed.; Academic Press: New York, 1974, Vol. 1; p 129; (b) Wortmann, R.; Elich, K.; Lebus, S.; Liptay, W.; Borowicz, P.; Grabowska, A. *J. Phys. Chem.* **1992**, *96*, 9724.

(41) We note that in the reference papers on EOA data,[10] a different value is reported for ACRI system in dioxane, namely 911×10^{-30} esu (or 338×10^{-50} CV^{-2} m^3); the value reported in Table 2 has been obtained directly by inserting experimental data of $\Delta\mu$, ΔE and μ^T into eq 1.

(42) Jørgensen, P.; Jensen, H. J. A.; Olsen, J. *J. Chem. Phys.* **1988**, *89*, 3654.

(43) (a) Frisch, M. J.; Head-Gordon, M.; Pople, J. *Chem. Phys. Lett.* **1990**, *166*, 275. (b) Frisch, M. J.; Head-Gordon, M.; Pople, J. *Chem. Phys. Lett.* **1990**, *166*, 281. (c) Head-Gordon, M.; Head-Gordon, T. *Chem. Phys. Lett.* **1994**, *220*, 122.

(44) Christiansen, O.; Jørgensen, P.; Hattig, C. *Int. J. Quantum Chem.* **1998**, *68*, 1.

(45) (a) Colwell, S. M.; Murray, C. W.; Handy, N. C.; Amos, R. D. *Chem. Phys. Lett.* **1993**, *109*, 261. (b) Lee, A. M.; Colwell, S. M. *J. Chem. Phys.* **1994**, *101*, 9704. (c) van Gisbergen, S. J. A.; Snijders, J. G.; Baerends, E. J. *J. Chem. Phys.* **1998**, *109*, 10644. (d) Salek, P.; Vahtras, O.; Helgaker, T.; Ågren, H. *J. Chem. Phys.* **2002**, *117*, 9630.

(46) (a) Cammi, R.; Cossi, M.; Tomasi, J. *J. Chem. Phys.* **1996**, *104*, 4611. (b) Cammi, R.; Cossi, M.; Mennucci, B.; Tomasi, J. *J. Chem. Phys.* **1996**, *105*, 10556. (c) Cammi, R.; Mennucci, B.; Pomelli, C.; Cappelli, C.; Corni, S.; Frediani, L.; Trucks, G. W.; Frisch, M. J. *Theor. Chem. Acc.* **2004**, *111*, 66.

(47) The FF results have been obtained using an applied electric field of 0.0033 au but checks with other fields have been also conducted without finding any significative differences in the resulting properties.

(48) (a) Willetts, A.; Rice, J. E.; Burland, D. M.; Shelton, D. P. *J. Chem. Phys.* **1992**, *97*, 7590. (b) Shi, R. F.; Garito, A. F. In *Characterization Techniques and Tabulations for Organic Nonlinear Optical Materials*; Kuzyk, M. G.; Dirk, C. W., Eds.; Dekker: New York, 1998; p 128; (c) Reis, H. *J. Chem. Phys.* **2006**, *125*, 014506.

(49) Orr, B. J.; Ward, J. F. *Mol. Phys.* **1971**, *20*, 513.

(50) Kuzyk, M. G. *Phys. Rev. A* **2005**, *72*, 053819.

(51) Champagne, B.; Kirtman, B. *J. Chem. Phys.* **2006**, *125*, 024101.

JP904906N